Vinorelbine-induced oxidative injury in human endothelial cells mediated by AMPK/PKC/NADPH/NF-κB pathways

Tsai et al: Vinorelbine-induced endothelial cell dysfunction

Kun-LingTsai[a], Tsan-Hung Chiu[b], Mei-Hsueh Tsai[c], Hsiao-Yun Chen[d], and Hsiu-Chung Ou[c]

a. Department of Physical Therapy and Graduate Institute of Rehabilitation Science, China Medical University, Taichung, Taiwan; b. Department of Obstetrics and Gynecology, China Medical University Hospital, Taichung, Taiwan; c. 3M Taiwan LTD. Health Care Business; d. Institute of Clinical Medicine, National Yang-Ming University, Taipei, Taiwan.

Correspondence to: Hsiu-Chung Ou, PhD, Department of Physical Therapy and Graduate Institute of Rehabilitation Science, China Medical University, Taichung,Taiwan No. 91, Shuch-Shih Road, Taichung 404, Taiwan

Fax: 886-4-22065051

Tel: 886-4-22053366 ext 7313

E-mail address: ouhc@mail.cmu.edu.tw

Abstract Vinorelbine tartrate (VNR), a semi-synthetic vinca alkaloid acquired from vinblastine, has extensively been used as an anticancer agent. However, VNR-induced oxidative damage may cause several side-effects, such as venous irritation, vascular pain and necrotizing vasculitis, thereby repressing clinical treatment efficiency. The molecular mechanisms underlying the induced oxidative stress in endothelial cells are still largely unknown. The present study was designed to test the hypothesis that VNR induces oxidative injury via modulation of AMP-activated protein kinase (AMPK) and possible mechanisms were then explored. Human umbilical vein endothelial cells (HUVECs) were treated with VNR (5-0.625 μM) to produce oxidative damage. The VNR-mediated AMPK, PKC and NADPH oxidase expression were investigated by Western blotting. Moreover, several oxidative stress-induced oxidative damage markers as well as pro-inflammatory responses were also investigated.VNR treatment resulted in dephosphorylation of AMPK, which in turn led to an activation of NADPH oxidase by PKC, however, the phenomena were repressed by AICAR (an agonist of AMPK) or AMPK siRNA. Moreover, VNR suppressed Akt/eNOS and enhanced p38 mitogen-activated protein kinase (MAPK), which in turn activated the NF-κB pathway. Furthermore, VNR facilitated several pro-inflammatory events, such as the adherence of monocytic THP-1 cells to HUVECs, pro-inflammatory cytokines release as well as over-expression of adhesion molecular. Our results highlight a possible

molecular mechanism for VNR-mediated endothelial dysfunction.

Highlights:

1. VNR-mediated endothelial cells dysfunction by increasing oxidative stress.
2. VNR-facilitated oxidative stress by repressing AMPK-α and activating PKC-αβ.
3. VNR-induced ROS production mainly go through NADPH oxidase activation.
4. Knockdown of AMPK impairs the VNR-induced PKC-αβ and p47phox activation.
5. VNR-induced endothelial cells inflammation by activating MAPKs and NF-κB pathway.

Key words: Vinorelbine tartrate, reactive oxygen species, endothelial cells, oxidative stress, AMPK

Abbreviations: Vinorelbine tartrate (VNR), reactive oxygen species (ROS), AMP-activated protein kinase (AMPK), protein kinase C (PKC), mitogen-activated protein kinase (MAPK), diphenyleneiodonium (DPI), ethylene diaminotetraacetic acid (EDTA), vascular cell adhesion molecule-1 (VCAM-1), intercellular adhesion molecules (ICAM-1), interleukin-8 (IL-8), nitric oxide (NO), endothelial NO synthase (eNOS)

Introduction

Vinca alkaloids remain among the most effective classes of anticancer drugs in clinical use [1]. Vinorelbine tartrate (VNR) is a semi-synthetic vinca alkaloid acquired from vinblastine. Vinorelbine has extensively been used as an anti-cancer or anti-angiogenesis drug in clinical strategies [2, 3]. VNR represses the polymerization of tubulin into microtubules and attenuates spindle formation by binding to tubulin [4, 5]. However, several side effects of VNR in clinical management have been reported, such as venous irritation, vascular pain, phlebitis, and necrotizing vasculitis [6]. Moreover, Yamada et al. demonstrated VNR-mediated human endothelial cell apoptosis through the induction of reactive oxygen species (ROS) production and repression of antioxidant enzyme function [7].

In endothelial cells, AMP-activated protein kinase (AMPK) plays a central role to maintain and detect intracellular homeostasis [8]. AMPK is also a well-known and important actor in modulating cellular energy balance and metabolism and responses to metabolic-related stress in endothelial cells [9], indicating that AMPK is functional and effective in repressing oxidative stress-mediated injury in endothelial cells. AMPK has several isoforms, including AMPK-α1,β1, and γ1 in endothelial cells, that manipulate multiple signal transduction pathways, with effects that include mitigating intracellular ROS formation, attenuating NADPH oxidase activation, reinforcing the

AKT pathway, and enhancing NO bioavailability [10, 11] . Moreover, Sag et al. demonstrated that AMPK plays a role as a cardiovascular protector by counteracting oxidative stress, inhibiting inflammatory responses, and activating eNOS expression in endothelial cells [12].

Previous studies have shown that protein kinase C (PKC) is downstream of AMPK, where inhibition of PKC expression contributes to the attenuation of NADPH oxidase-derived ROS production [13]. NADPH oxidase is comprised of membrane-bound gp91phox and p22hox, as well cytosolic subunits such as p47phox, p67phox, and the small GTPase Rac. Endothelial NADPH oxidase-derived ROS generation appears to be a driving force in the development of endothelial dysfunction and cardiovascular disease, indicating that NADPH oxidase-activated ROS act as a secondary messenger to initiate downstream signal transduction pathways [14, 15], such as activation of p38 mitogen-activated protein kinase (MAPK), stimulation of nitric oxide (NO) catabolism as a result of superoxide generation, and inhibition of NO release via attenuated endothelial NO synthase (eNOS) [16], thereby activating NF-κB, which in turn triggers downstream pro-inflammatory responses[17, 18]

In clinical chemotherapy intervention, endothelial cells injury may contribute to vascular dysfunction and decrease treatment efficiency [19]. Yamada et al. showed that VNR-induced endothelial apoptosis was facilitated by ROS generation and

eliminated antioxidant enzyme expression. However, the detailed mechanisms of VNR-mediated injury in human endothelial cells are still unclear. In this study, we hypothesize that VNR-mediated oxidative damage is modulated by AMPK, increasing PKC and NADPH oxidase activation, thereby facilitating ROS generation, decreasing AKT/eNOS expression and increasing the NF-κB-mediated pro-inflammatory response.

Materials and Methods

Reagents. Fetal bovine serum, M199, and trypsin-EDTA were obtained from Gibco (Grand Island, NY, USA). Low serum growth supplement was obtained from Cascade (Portland, OR). Vinorelbine, diphenyleneiodonium (DPI), ethylene diaminotetraacetic acid (EDTA), pyrrolidine dithiocarbamate (PDTC), metformin, penicillin, and streptomycin were obtained from Sigma (St. Louis, MO). SB203580 and compound C were purchased from Calbiochem (CA, USA). Anti-vascular cell adhesion molecule-1 (VCAM-1), anti-intercellular adhesion molecules (ICAM-1), anti-E-selectin, and Interleukin-8 (IL-8) ELISA kits were purchased from R&D Systems (Minneapolis, MN). Anti-p22phox and anti-gp91 were obtained from Santa Cruz (CA, USA), and anti-NF-κB/p65, anti-IκBα, anti-AMPK, anti-AMPK-α, anti-AKT, anti-phospho AKT, anti-phospho eNOS, anti-eNOS, anti-PCNA, anti-phospho p38, anti-p38, anti-PKC, and anti-phospho PKCαβ were obtained from Transduction Laboratories (CA, USA). Anti-Rac-1 and anti-p47phox were obtained from BD Biosciences (NJ, USA). Anti-cyclooxygenase-2 (COX-2) was obtained from Chemicon (MA, USA).

Cell cultures. These experiments were approved by the Research Ethics Committee of the China Medical University Hospital. After receiving written

informed consent from the parents, fresh human umbilical cords were obtained from neonates after birth, collected and suspended in Hanks' Balanced Salt Solution (HBSS) (Gibco, USA) at 4°C. Human umbilical vein endothelial cells (HUVECs) were isolated with collagenase and used at passage 2-3 [20]. After dissociation, the cells were collected and cultured on gelatin-coated culture dishes in medium 199 with low serum growth supplement, 100 IU/mL penicillin, and 0.1 mg/mL streptomycin. Subcultures were performed with trypsin-EDTA. Media were refreshed every two days.

Total RNA isolation and real-time PCR reaction. To investigate the effects of VNR-induced adhesion molecule gene expression in endothelial cells, HUVECs were incubated with VNR for 24 hours. Total RNA was isolated using TRIzol reagent. Reverse transcription was performed at 42°C for 60 min, followed by incubation at 95°C for 5 min. The reaction 20 mixture (20 μl of total volume) consisted of 2 μg of isolated total RNA, 1 mM dNTP, 1 unit/μl of recombinant RNasin ribonuclease inhibitor, 15 U/μg of avian myeloblastosis 22 virus (AMV) reverse transcriptase, 5× RT buffer, and 0.5 μg of oligo(dT)12 primer. The gene-specific primers used were as follows:

ICAM-1 sense: 5’-CCGAGCTCAAGTGTCTAAAG-3’; ICAM-1 antisense:

5’-TGCCACCAATATGGGAAGGC-3’; VCAM-1 sense:

5’-AAGATGGTCGTGATCCTTGG-3’; VCAM-1 antisense:

5’-GGTGCTGCAAGTCAATGAGA-3’; E-selectin sense:

5’-AGCTTCCCATGGAACACAAC-3’; E-selectin antisense:

5’-CTGGGCTCCCATTAGTTCAA-3’; β-actin sense:

5’-GGACTTCGAGCAAGAGATGG-3’; and β -actin antisense:

5’-AGCACTGTGTTGGCGTACAG-3’. Real-time PCR reactions were performed using the SYBR Green method in an ABI 7000 sequence detection system (Applied Biosystems, Foster City, CA) following the manufacturer's guidelines. Primers were designed using the computer software Primer Express 2.0 (Applied Biosystems, Foster City, CA). The reactions were set by mixing 12.5 μl of the SYBR Green Master Mix (Applied Biosystems, Foster City, CA) with 1 μl of a solution containing 10 μM concentrations of both primers and 2 μl of cDNA solution. The Ct value was defined as the number of PCR cycles required for the fluorescence signal to exceed the detection threshold value. The relative amounts of mRNA for each gene were normalized based on the amount of the housekeeping gene β-actin.

Measurement of ROS production. HUVECs (10^4 cells/well) in 96-well plates were pre-incubated with 10 μM DCF-AM for 1 h; the fluorescence intensity was

measured with a fluorescence microplate reader (Labsystems, CA, USA) calibrated for excitation at 485 nm and emission at 538 nm (before and after 24 hours of stimulation with various concentrations of VNR), The percentage increase in fluorescence per well was calculated by the formula $[(Ft_2-Ft_0)/Ft_0]$ X 100, where Ft_2 is the fluorescence at at each time (15, 30, 60, 120 mins) of VNR exposure and Ft_0 is the fluorescence at 0 min of VNR exposure.

Transfection with small interfering RNA (siRNA). ON-TARGETplus SMARTpool siRNAs for non-targeting controls and NF-κBp65 siRNAs were purchased from Dharmacon. Three days after transfection, cells were treated with the indicated reagent for further experiments.

Preparation of nuclear and cytosolic extracts. Nuclear and cytosolic extracts were isolated with a Nuclear and Cytoplasmic Extraction kit (Pierce Chemical, Rockford, IL). After the incubation period, HUVECs were collected by centrifugation at 600 g for 5 min at 4°C. The pellets were washed twice with ice-cold PBS, followed by the addition of 0.2 ml of cytoplasmic extraction buffer A and vigorous mixing for 15 s. Ice-cold cytoplasmic extraction buffer B (11μl) was added to the solution. After vortex mixing, nuclei and cytosolic fractions were separated by centrifugation at 16,000 g for 5 min. The cytoplasmic extracts (supernatants) were stored at -80°C. Nuclear extraction buffer was added to the nuclear fractions (pellets), which were then mixed by vortex mixing on the highest setting for 15 s. The mixture was iced, and a 15-s vortex was performed every 10 min for a total of 40 min. Nuclei were centrifuged at 16,000 g for 10 min. The nuclear extracts (supernatants) were stored at -80°C until use.

Preparation of membrane and cytosolic extracts. A cellular membrane fraction was prepared with Mem-PER (Pierce) according to the manufacturer's instructions. The Mem-PER system consists of three reagents: reagent A is a cell lysis buffer, reagent B is a detergent dilution buffer, and reagent C is a membrane solubilization buffer. After the incubation period, HUVECs were collected by centrifugation at 600 g for 5 min at 4°C. Each cell pellet, containing $5x10^6$ cells, was lysed at room temperature using Mem-PER reagent A. Membrane proteins were solubilized on ice with Mem-PER reagent C diluted 2:1 with Mem-PER reagent B. Reagents A and B/C were supplemented with Halt protease inhibitor cocktail (Pierce Biotechnology). The solubilized protein mixture was centrifuged at 10,000 g for 3 min at 4°C to remove cellular debris. The clarified supernatant was heated at 37°C for 10 min, followed by centrifugation at 10,000 g for 2 min to produce separated membrane and hydrophilic protein fractions. The hydrophobic fraction of the membrane proteins (bottom layer) was stored at -80°C until use.

Protein kinase C-α assay. HUVECs were grown to confluence and then stimulated with VNR for 1 hour. At the end of the incubation period, cells were rinsed with ice-cold PBS and lysed by the addition of reaction buffer (50 mM HEPES, pH 7.2, 0.01% BSA, 10 mM MgCl2, 1 mM DTT, and 1x lipid activator, provided in the kit). Protein kinase C-α activity in wholecell lysate (10 µg) was measured with a PKC-α activity assay kit (nonradioactive) according to the manufacturer's

instructions (Upstate Biotechnology).

Immunoblotting. To determine how VNR-mediated signaling pathways are altered, HUVECs were incubated with VNR for 24 hours. At the end of stimulation, cells were washed, scraped from dishes, and lysed in RIPA buffer. Proteins were then separated by electrophoresis on SDS-polyacrylamide gels. After the proteins had been transferred to polyvinylidene difluoride membranes (Millipore, Bedford, MA), the blots were incubated with blocking buffer for 1 h at room temperature and then probed with primary antibodies overnight at 4℃, followed by incubation with horseradish peroxidase-conjugated secondary antibody for 1 h. To control for unequal loading of total protein in all lanes, blots were stained with mouse anti−β-actin antibody. The bound immunoproteins were detected via an enhancer chemiluminescent assay (ECL; Amersham, Berkshire, UK). The intensities were quantified by densitometric analysis (Digital Protein DNA Imagineware, Huntington Station, NY).

Adhesion molecule expression. To determine whether VNR could enhance the level of adhesion molecule expression, HUVECs were incubated with VNR for 24 hours. Following stimulation, HUVECs were harvested and incubated with

fluorescence-conjugated anti-ICAM-1, anti-VCAM-1, and anti-E-selectin (R&D, Minneapolis, MN) for 45 min at room temperature. After the HUVECs had been washed three times, their immunofluorescence intensity was analyzed by flow cytometry using a Becton Dickinson FACScan flow cytometer (Mountain View, CA).

Adhesion assay. HUVECs at $1X10^5$ cells/mL were cultured in 96-well plates. HUVECs were incubated with VNR for 24 hours. The medium was then removed, and 0.1 mL/well of THP-1 cells (prelabeled with 4 μM BECF-AM for 30 min in RPMI at $1X10^6$ cells/mL density) were added to fresh RPMI. The cells were allowed to adhere at 37◦C for 1 h in a 5% CO_2 incubator. Plates were washed three times with M199 to remove the non-adherent cells. The number of adherent cells was estimated by microscopic examination, and the cells were then lysed with 0.1 mL 0.25% Triton X-100. Fluorescence intensity was measured with a fluorescence microplate reader (Labsystem, CA) calibrated for excitation at 485 nm and for emission at 538 nm.

Assay for IL-8 secretion. HUVECs were seeded in 24-well plates at 0.5×10^5 cells. After 2 days, HUVECs were incubated with VNR for 24 hours. At the end of the VNR incubation period, cell supernatants were removed and assayed for

IL-8 concentration using an ELISA kit obtained from R&D Systems (Minneapolis, MN). Data are expressed as ng/mL for duplicate samples.

Statistical analyses. Results are expressed as mean±SEM. Differences between groups were analyzed using one-way ANOVA followed by Bonferroni's post hoc test. A P-valueb0.05 was considered statistically significant.

Results

VNR induced dephosphorylation of AMPK-α, phosphorylation of PKC-αβ as well as PKC-α activity. AMPK can reverse and alter many cellular pathways to protect against oxidative injury [21]. We assumed that VNR-induced endothelial cell dysfunction was caused by repression of AMPK phosphorylation. To verify our hypothesis, the protein expression level of phosphorylated AMPK was determined using a Western blotting assay. As shown in Fig. 1A and 1B, treatment of HUVECs with VNR for 1 hour led to an attenuation of phosphorylated AMPK-α in a dose-dependent manner.

Moreover, previous studies have shown that PKC isoforms play a key role in the regulation of NADPH subunit expression and, in particular, the translocation of $p47^{phox}$ from the cytosol to the membrane [22, 23], and AMPK-α can inhibit ROS production via suppression of protein kinase C (PKC), which in turn prevents the activation of NADPH oxidase [13]. We therefore focused our attention on determining whether VNR facilities PKC phosphorylation and activation in human endothelial cells. As shown in Fig. 1C and 1E, VNR markedly increased phosphorylation of PKC-αβ and PKC-α activity after a 1 h exposure. Pretreatment of AICAR, one agonist of AMPK, significantly mitigated VNR-promoted

phosphorylation of PKC-αβ and PKC-α activity, indicating that PKC is implicated in VNR-induced endothelial cell injury and mainly go through AMPK.

VNR induced membrane assembly of NADPH. A previous study revealed that VNR induces ROS formation in endothelial cells, thereby facilitating endothelial cell apoptosis[7]. We proposed that VNR facilitates ROS production mainly by promoting PKC phosphorylation and activating NADPH oxidase. DPI, an inhibitor of NADPH oxidase, was used to prove our hypothesis. In endothelial cells, the NOX family of NADPH oxidases is an important source of ROS generation. NADPH oxidase is composed of two membrane components, Nox2 (also called gp91phox) and p22phox, and three cytoplasmic components, p47phox, p67phox, and the small GTPase Rac-1. The process by which the NADPH oxidase enzyme complex is activated begins with the phosphorylation of p47phox, which causes translocation of the p47 phox /p67phox complex to the plasma membrane, where p47phox interacts with p22phox and p67phox acts as a NOX activator through a direct protein-protein interaction. Therefore, we verified the effects of NADPH oxidase activation after exposure to VNR. The membrane translocation assay showed that the levels of p47phox and Rac-1 in membrane fractions of HUVECs were higher in cells treated with VNR for 1 hour than control cells. In addition, we found that the protein levels of gp91 and p22

phox were increased significantly in HUVECs exposed to VNR for 24 hours. Moreover, pretreatment of VNR-exposed cells with AICAR led to a reduction in membrane assembly of $p47^{phox}$ and Rac-1, as well as suppression of gp91 and $p22^{phox}$ protein expression (Fig. 2A-C).

VNR-induced intracellular ROS generation in HUVECs. Fluorescence intensity were measured to clarify whether the VNR-promoted intracellular ROS formation in human endothelial cells. As Fig.3, our data showed that exposure to VNR for 2 hours resulted in an increasing of ROS in a dose-dependent manner. In addition, pre-treatment with DPI and AICAR abrogated the VNR-elicited ROS generation, suggesting that ROS generation were largely dependent on the repressing AMPK function and the subsequent activation of NADPH oxidase.

VNR mediated oxidative injury involves Akt/eNOS deactivation. Akt serves a major role in promoting cell survival in response to various death stimuli. Moreover, Akt activates endothelial nitric oxide synthase (eNOS), which leads to nitric oxide (NO) production**.** Studies have reported that oxidative stress decreases Akt and eNOS phosphorylation in endothelial cells [24], while activation of Akt and eNOS are known to repress apoptosis and promote cell survival [25]. To investigate whether

AMPK/Akt/eNOS signaling is involved in the impaired effects of VNR, we performed a Western blot analysis using phosphor-specific Akt (Ser473) and phosphor-eNOS (Ser1177) antibodies. As expected, VNR significantly lessened the phosphorylation of Akt and eNOS in a dose-dependent manner (Fig 4). Pretreatment of AICAR manifestly restored the expression level of phosphorylated Akt and eNOS. This finding suggested that AMPK/Akt/eNOS signaling is involved in the VNR-induced oxidative injuries. Moreover, pretreatment DPI also reduced VNR-repressed Akt and eNOS phosphorylation. This result suggesting that the NADPH oxidase-derived ROS play an important role to repress Akt and eNOS function, thereby inducing endothelial cells oxidative damage.

VNR induced ERK activation and decreased PPAR-γ expression. ERK signaling plays an essential role in oxidative stress-mediated signaling. Peroxisome proliferator-activated receptors (PPARs) comprise a superfamily of nuclear hormone receptor proteins that function as transcription factors. Activation of PPAR-γ has been displayed to repress expression of pro-inflammatory mediators such as cyclooxygenase-2 (COX-2) and NF-κB [26, 27]. We next focused our attention on determining whether VNR facilitates endothelial cell dysfunction by activating ERK phosphorylation and attenuating PPAR-γ expression. As shown in Fig. 5, treatment of

VNR markedly activated ERK phosphorylation and decreased PPAR-γ expression. Nevertheless, pretreatment with AICAR suppressed the phenomenon. The results were support out hypothesis. VNR increases ERK phosphorylation and decreases PPAR-γ function by modulating AMPK expression. Pretreatment of DPI also protected against VNR- activated ERK phosphorylation and decreased PPAR-γ expression, revealing that the NADPH oxidase-derived ROS are key mediator involved in this signaling.

VNR induced NF-κB activation by modulation of p38MAPK. Oxidative stress-mediated ROS can mediate p38MAPK and phosphoinositide 3-kinase (PI3K) activation, and both of these mediators cause NF−κB activation, which facilitates nuclear translocation and subsequent manipulation of pro-inflammatory events [2]. As shown in Fig. 6A, VNR clearly induced p38MAPK phosphorylation as compared to control cells. However, pre-treatment with SB203580, a specific inhibitor of p38MAPK, decreases the phosphorylation level of p38MAPK. NF-κB is an important mediator of pro-inflammatory pathways. When pro-inflammatory responses are activated, NF-κB dissociates from the inhibitor factor I-κB and subsequently translocates to the nucleus, where it exists primarily as a p65/p50 heterodimer and binds directly to its cognate DNA sequence. As shown in Fig. 6A, after exposure to

VNR, I-κB was degraded, thereby causing nuclear translocation of NF-κBp65. In contrast, in cells pretreated with SB203580, VNR-induced NF-κB activation was markedly inhibited.

VNR increased the NF-κB-related pro-inflammatory response in HUVECs.

NF-κB is a vital player in regulation of the inflammatory response, apoptosis, and cell survival [28]. Pro-inflammatory cytokines, cyclooxygenase II (COX-II), and adhesion molecules are modulated by NF-κB, with pro-inflammatory events subsequently leading to the tethering and adherence of monocytic cells to endothelial cells. Our results show that treatment with VNR facilitated the expression of COX-II (Fig.7A, 7B), increased the expression of adhesion molecules (ICAM-1, VCAM-1 and E-selectin) based on protein levels (Fig. 7D) and the mRNA levels (Fig. 7E), and the adhesion of monocytic THP-1 cells to HUVECs (Fig. 7F), and increased the secretion of IL-8 (Fig. 7G). To further investigated whether NF-κB plays a major role in VNR-induced endothelial cells inflammation, we used a NF-κBp65 siRNA and examined the changes of the pro-inflammatory responses. Our results showed that NF-κBp65 siRNA and the NF-κB inhibitor (PDTC) significantly antagonized the VNR-facilitated pro-inflammatory events, indicating that VNR promoted endothelial inflammation majorly by activating NF-κB.

Metformin, a clinical drug, is one of the most familiarly compound to promote AMPK function [29], we used metformin and AICAR to investigate whether AMPK agonist reduces VNR- derived inflammatory responses. As expect, both of metformin and AICAR effectively mitigate VNR- derived inflammatory responses (Fig. 7A-7E).

Discussion

In clinical practice, vinorelbine has widely used as an anti-cancer drug. Several side effects have been revealed, such as phlebitis [6]. A previous study showed that VNR induces ROS generation, thereby facilitating downstream pro-apoptotic responses, such as collapsed mitochondrial membrane potential and increased phosphatidylserine translocation [7] . In this present study, we first demonstrated that VNR induces ROS generation and oxidative injury by modulating AMPK/PKC/NADPH oxidase. Our data shows that VNR elicited dephosphorylation of AMPK, which led to PKC-αβ-mediated NADPH oxidase activation and subsequent superoxide generation, as well as impaired Akt/eNOS signaling. VNR increased ERK activation, which contributed to repression of PPAR-γ expression. Moreover, VNR activated p38MAPK expression and NF-κB- mediated pro-inflammatory events.

AMPK acts as a detector of cellular homeostasis and also modulates oxidative stress [8]. AMPK can also mediate several signaling cascades, leading to the repression of free radical generation and the activation of angiogenic factors. Several lines of evidence have demonstrated that PKC, which is negatively regulated by AMPK, is required for the activation of NADPH oxidase, and the inhibition of PKC contributes to the attenuation of NADPH oxidase-derived ROS production [13].

Amassing research supports that AMPK negatively regulates PKC, which in turn mediates diverse signaling pathways. For example, palmitic acid-activated endothelial CRP expression involves PKC-facilitated oxidative injury by repressing AMPK expression level [30]. Cellotto et al published the rosiglitazone enhances AMPK function, in turn, protects against high glucose-induced hyperactivity of NADPH oxidase by inhibiting PKC [13]. Moreover, AMPK has been considered as a protector of the cardiovascular system by enhancing NO bioavailability [11]. Our data confirmed that VNR induces de-activation of AMPK and activation of PKC (Fig.1). Moreover, AMPK supports endothelial function by repressing NADPH oxidase-derived superoxide production [31]. NADPH oxidase consists of membrane-bound gp91phox and p22hox, as well cytosolic subunits such as p47phox, p67phox, and the small GTPase Rac. Endothelial NADPH oxidase-derived ROS generation appears to be a driving force in the development of endothelial dysfunction and cardiovascular diseases, indicating that NADPH oxidase-activated ROS act as a secondary messenger to turn on downstream signal transduction pathways leading to endothelial cell dysfunction [14, 15]. Our results suggest that VNR enriches NADPH oxidase activation (Fig. 2). These findings are in agreement with previous studies that demonstrated that AMPK acts as a negative regulator of NADPH oxidase. For example, AMPK negatively regulates NOX4-dependent activation of p53 and

epithelial cell apoptosis [32], in addition to preventing the serine phosphorylation and membrane translocation of $p47^{phox}$ [33]. Those important finding revealed that VNR-mediated oxidative damage is regulated by the AMPK/PKC/NADPH oxidase pathway.

The caspase pathway is an important modulator of apoptosis and a well-identified downstream target for Akt/eNOS. One mechanism by which Akt/eNOS regulates cell survival involves the S-nitrosylation of cysteine 163 in the active center of the catalytic subunit p17 of caspase-3, resulting in inhibition of its activity. Our data revealed that VNR repressed AKT and eNOS phosphorylation (Fig. 4). Moreover, a previous study reported that VNR induces endothelial cell apoptosis by activating caspase 3 [7], suggesting that VNR activates caspase 3 expression by decreasing AKT and eNOS phosphorylation.

Peroxisome proliferator-activated receptors (PPARs) are nuclear receptors and are able to modulate gene expression and activation via binding with the retinoid X receptor as a heterodimeric partner to specific DNA sequence elements[34]. Moreover, PPARs have been shown to affect lipid and glucose metabolisms. PPAR-γ is expressed in endothelial cells and is inhibited by MAPK-mediated signaling [35]. PPAR-γ protects against TNF-α-mediated adhesion molecular expression [36, 37], suggesting that PPAR-γ may play a role in suppressing the generation and progression

of oxidative injury by modulating metabolic disorders and modifying pro-inflammatory reactions in human endothelial cells. Our data revealed that VNR facilitated ERK activation and inhibited PPAR-γ expression (Fig. 5), thereby inducing endothelial cell damage. Moreover, pretreatment with AICAR evidently reversed the VNR-repressed PPAR-γ expression level, indicating that VNR-repressed PPAR-γ expression mainly by regulating AMPK activity.

ROS can be a secondary signaling mediator to regulate signal transduction. Both the MAPK and PI-3K pathways are involved in oxidative stress-activated NF-κB translocation [38], which may be a critical mechanism in endothelial inflammation. NF-κB was one of the key mediator of adhesion molecules at the transcriptional level in human vascular endothelial cells [39]. In this article, SB203580 observably attenuates I-κB degradation as well as NF-κB p65 translocation, indicating a promotion of VNR-induced NF-κB p65 expression by enhancing p38MAPK activation (Fig.6).

Inflammation mediated by overexpression of adhesion molecules and cytokines is reported to participate to the pathogenesis of endothelial cells dysfunction. ICAM-1, VCAM-1 as well as E-selectin are adhesion molecules of endothelial cells, they have been validated to be up-regulated in the endothelial cells of oxidative damage, the activation of the molecules might promote growth factor production and medial

smooth muscle cells migration [40]. Hattory et al reported the AMPK activator, metformin, protects against TNF-α-induced NF-κB p65 activation an adhesion molecules up-expression [41], supporting that oxidative stress-caused NF-κB p65 activation an adhesion molecules overexpression by impairing AMPK function. In our study, NF-κBp65 siRNA, PDTC, AICAR and metformin manifestly antagonized the VNR-activated adhesion molecules expression as well as pro-inflammation responses, such as IL-8 secretion, adhesion molecule expression and monocyte attachment (Fig.7), exhibiting the VNE-derived endothelial cells inflammation via weakening AMPK and activating NF-κB.

VNR is very lipophilic and can be rapidly distributed by peripheral tissue. After intravenous injection of 30-30 mg/m^2 VNR, a plasma concentration of 1 μM is quickly reached [42]. In the present study, the VNR concentrations we used (5-0.625 μM) are very similar to those from other studies. For example, Yamada et al. reported that 3 μM VNR is able to induce ROS generation and apoptotic expression [7]. Moreover, our data shows that 1.25 μM VNR, which may be achieved under human physiological conditions, can induce endothelial cell oxidative injury, increase NADPH oxidase activation, and repress eNOS and PPAR–γ expression, facilitated by p38MAPK and NF-κB activation.

In summary, in this study we demonstrate for the first time VNR-induced

oxidative injury caused by repression of AMPK function, increased PKC and NADPK oxidase activation, attenuation of AKT/eNOS expression, enhanced ERK phosphorylation, decreased PPAR-γ expression, and activation of NF-κB expression, all concomitantly triggering the pro-inflammatory response in endothelial cells (Fig.8).

Acknowledgements

This study was supported by grants from The National Science Council, (NSC 98-2320-B-039-020-MY3, NSC 97-3111-B-075-001-MY3, 97-2320-B-075-003-MY3), China Medical University (CMU99-S-13), Taiwan, ROC. This study was supported in part by Taiwan Department of Health Clinical Trial and Research Center of Excellence (DOH100-TD-B-111-004)

Figure legends

Figure 1. VNR repressed endothelial AMPK activation (A, B),induced PKC activation (C-D). HUVECs were exposed to VNR (0.625-5 μM) for 1 hours. At the end of the incubation period, levels of phosphorylated AMPK and PKC were determined by immunoblotting. The protein levels of p-AMPK-α were normalized to the level of AMPK-α. The protein levels of p-PKCα/β were normalized to the level of PKC. (E) PKC-α activity in whole-cell lysates was measured by a fluorescein green assay kit. Data are the mean±SE of three different experiments. #P<0.05 compared with untreated control HUVECs. *P<0.05 compared with 5 μM VNR-stimulated HUVECs.

Figure 2. VNR increased the level of NADPH oxidase membrane assembly. HUVECs were stimulated for 2 hours with the indicated concentrations of VNR. In one sample, HUVECs were pretreated with AICAR for 1 hour before exposure to VNR. Preparation of membrane and cytosolic proteins is described in the Materials and Methods section. Representative Western blots (A) and summary data (B, C) showed that VNR induced $p47^{phox}$ and Rac-1 translocation to the plasma membrane, as well as gp91 and $p22^{phox}$ expression. The levels of cytosolic protein and membrane protein

were normalized to the levels of β-actin and flotillin-1, respectively. Data are the mean±SE of three different experiments. #P<0.05 compared with untreated control HUVECs. *P<0.05 compared with 5 μM VNR-stimulated HUVECs.

Figure 3. Time course of VNR-induced ROS generation in HUVECs. After pre-incubation for 2 hours with the DPI (NADPH oxidase inhibitor) or AICAR(AMPK agonist). After pre-incubation for Cells were treated with various concentrations of VNR followed by 1 hour incubation with DCF-AM. Fluorescence intensity of cells was measured with a fluorescence microplate reader. Data are means±SE of 3 different experiments. #P<0.05 compared with untreated control HUVECs. *P<0.05 compared with VNR-stimulated HUVECs.

Figure 4. VNR down-regulated Akt and eNOS activation (A-C). HUVECs were stimulated for 2 hours with the indicated concentrations of VNR. In one sample, HUVECs were pretreated with DPI or AICAR for 1 hour before exposure to VNR. At the end of the incubation period, the levels of phosphorylated Akt and eNOS were determined by immunoblotting. Data are the mean±SE of three different experiments. #P<0.05 compared with untreated control HUVECs. *P<0.05 compared with 5 μM VNR-stimulated HUVECs.

Figure 5. VNR facilitated endothelial ERK activation and inhibition of PPAR-γ expression (A-C). HUVECs were exposed to the indicated concentrations VNR for 1 hour (ERK) or 24 hours (PPAR-γ). In one sample, HUVECs were pretreated with DPI or AICAR for 1 hour before exposure to VNR. At the end of the incubation period, the levels of phosphorylated ERK and PPAR-γ were determined by immunoblotting. The protein levels of p-ERK were normalized to the level of ERK. The protein levels of PPAR-γ were normalized to the level of β-actin. Data are the mean±SE of three different experiments. #P<0.05 compared with untreated control HUVECs. *P<0.05 compared with 5 μM VNR-stimulated HUVECs.

Figure 6. VNR activated p38 MAPK phosphorylation and increased the translocation of NF-κB. HUVECs were stimulated for 2 hours with the indicated concentrations of VNR. In some samples, HUVECs were pretreated with DPI or SB203580 for 1 hour before exposure to VNR (A-D). Western blot analysis was used to evaluate the expression of both phosphorylated and total p38 MAPK (B) and the activation of NF-κB. Anti-β-actin and anti-PCNA antibodies were used for normalization of cytosolic and nuclear proteins (C, D), respectively. Data are the mean±SE of three different experiments. #P<0.05 compared with untreated control HUVECs. *P<0.05

compared with 5 μM VNR-stimulated HUVECs.

Figure 7. VNR activated NF-kB-related pro-inflammation responses. VNR increased COX-II expression (A,B). HUVECs were stimulated for 24 hours with the indicated concentrations of VNR. HUVECs were pretreated with PDTC or AICAR or metformin for 1 hour before exposure to VNR. In some sample, transfected with NF-κBp65 siRNA or si-Control for 48 h followed by exposure to VNR. Western blot analysis was used to evaluate the si-NF-κBp65 knockdown efficiency (C) and the expression of COX-II, and Anti-β-actin antibodies were used for normalization of protein expression level. VNR enhanced adhesion molecule expression at the mRNA level (D) and the protein level (E) and increased IL-8 release (R). mRNA levels of ICAM-1, VCAM-1 and E-selectin were determined by real-time PCR. Cell surface expression of ICAM-1, VCAM-1, and E-selectin were determined by flow cytometry. The protein level of VNR-induced IL-8 release was determined by ELISA. VNR increased attachment of THP-1 monocytic cells to HUVECs (G). THP-1 cells preloaded with BECEF were incubated with HUVECs for 1 h. The adhesiveness of HUVECs to THP-1 was measured as described in the Materials and Methods. #P<0.05 compared with untreated control HUVECs. *P<0.05 compared with 5 μM VNR-stimulated HUVECs.

Figure 8. Schematic diagram showing the signaling of VNR-induced endothelial oxidative injury. As depicted, VNR induces AMPK-α de-activation, PKCα/β phosphorylation, NADPH oxidase activation, and activated oxidative stress-related signal transduction pathways. The → indicates activation or induction, and ┤ indicates inhibition or blockade.

References

1. Budman DR: **New vinca alkaloids and related compounds**. *Semin Oncol* 1992, **19**(6):639-645.
2. Marty M, Extra JM, Dieras V, Giacchetti S, Ohana S, Espie M: **A review of the antitumour activity of vinorelbine in breast cancer**. *Drugs* 1992, **44 Suppl 4**:29-35; discussion 66-29.
3. Sorensen JB: **Vinorelbine. A review of its antitumour activity in lung cancer**. *Drugs* 1992, **44 Suppl 4**:60-65; discussion 66-69.
4. Jordan MA, Wilson L: **Microtubules as a target for anticancer drugs**. *Nat Rev Cancer* 2004, **4**(4):253-265.
5. Ngan VK, Bellman K, Hill BT, Wilson L, Jordan MA: **Mechanism of mitotic block and inhibition of cell proliferation by the semisynthetic Vinca alkaloids vinorelbine and its newer derivative vinflunine**. *Mol Pharmacol* 2001, **60**(1):225-232.
6. Rittenberg CN, Gralla RJ, Rehmeyer TA: **Assessing and managing venous irritation associated with vinorelbine tartrate (Navelbine)**. *Oncol Nurs Forum* 1995, **22**(4):707-710.
7. Yamada T, Egashira N, Imuta M, Yano T, Yamauchi Y, Watanabe H, Oishi R: **Role of oxidative stress in vinorelbine-induced vascular endothelial cell injury**. *Free Radic Biol Med* 2010, **48**(1):120-127.
8. Dong Y, Zhang M, Wang S, Liang B, Zhao Z, Liu C, Wu M, Choi HC, Lyons TJ, Zou MH: **Activation of AMP-activated protein kinase inhibits oxidized LDL-triggered endoplasmic reticulum stress in vivo**. *Diabetes* 2010, **59**(6):1386-1396.
9. Hardie DG: **AMP-activated/SNF1 protein kinases: conserved guardians of cellular energy**. *Nat Rev Mol Cell Biol* 2007, **8**(10):774-785.
10. Fisslthaler B, Fleming I: **Activation and signaling by the AMP-activated protein kinase in endothelial cells**. *Circ Res* 2009, **105**(2):114-127.
11. Michell BJ, Chen Z, Tiganis T, Stapleton D, Katsis F, Power DA, Sim AT, Kemp BE: **Coordinated control of endothelial nitric-oxide synthase phosphorylation by protein kinase C and the cAMP-dependent protein kinase**. *J Biol Chem* 2001, **276**(21):17625-17628.
12. Sag D, Carling D, Stout RD, Suttles J: **Adenosine**

5'-monophosphate-activated protein kinase promotes macrophage polarization to an anti-inflammatory functional phenotype. *J Immunol* 2008, **181**(12):8633-8641.

13. Ceolotto G, Gallo A, Papparella I, Franco L, Murphy E, Iori E, Pagnin E, Fadini GP, Albiero M, Semplicini A *et al*: **Rosiglitazone reduces glucose-induced oxidative stress mediated by NAD(P)H oxidase via AMPK-dependent mechanism**. *Arterioscler Thromb Vasc Biol* 2007, **27**(12):2627-2633.
14. Griendling KK, Sorescu D, Ushio-Fukai M: **NAD(P)H oxidase: role in cardiovascular biology and disease**. *Circ Res* 2000, **86**(5):494-501.
15. Li JM, Shah AM: **Endothelial cell superoxide generation: regulation and relevance for cardiovascular pathophysiology**. *Am J Physiol Regul Integr Comp Physiol* 2004, **287**(5):R1014-1030.
16. Sugimoto K, Ishibashi T, Sawamura T, Inoue N, Kamioka M, Uekita H, Ohkawara H, Sakamoto T, Sakamoto N, Okamoto Y *et al*: **LOX-1-MT1-MMP axis is crucial for RhoA and Rac1 activation induced by oxidized low-density lipoprotein in endothelial cells**. *Cardiovasc Res* 2009, **84**(1):127-136.
17. Li D, Mehta JL: **Intracellular signaling of LOX-1 in endothelial cell apoptosis**. *Circ Res* 2009, **104**(5):566-568.
18. Navarra T, Del Turco S, Berti S, Basta G: **The lectin-like oxidized low-density lipoprotein receptor-1 and its soluble form: cardiovascular implications**. *J Atheroscler Thromb* 2010, **17**(4):317-331.
19. Tesfamariam B, DeFelice AF: **Endothelial injury in the initiation and progression of vascular disorders**. *Vascul Pharmacol* 2007, **46**(4):229-237.
20. Jaffe EA, Nachman RL, Becker CG, Minick CR: **Culture of human endothelial cells derived from umbilical veins. Identification by morphologic and immunologic criteria**. *J Clin Invest* 1973, **52**(11):2745-2756.
21. Hardie DG, Carling D: **The AMP-activated protein kinase--fuel gauge of the mammalian cell?** *Eur J Biochem* 1997, **246**(2):259-273.
22. Bey EA, Xu B, Bhattacharjee A, Oldfield CM, Zhao X, Li Q, Subbulakshmi V, Feldman GM, Wientjes FB, Cathcart MK: **Protein kinase C delta is required for p47phox phosphorylation and translocation in activated human monocytes**. *J Immunol* 2004, **173**(9):5730-5738.
23. Ceolotto G, Papparella I, Lenzini L, Sartori M, Mazzoni M, Iori E, Franco L, Gallo A, de Kreutzenberg SV, Tiengo A *et al*: **Insulin generates free radicals in human fibroblasts ex vivo by a protein kinase C-dependent mechanism,**

which is inhibited by pravastatin. *Free Radic Biol Med* 2006, **41**(3):473-483.

24. Chavakis E, Dernbach E, Hermann C, Mondorf UF, Zeiher AM, Dimmeler S: **Oxidized LDL inhibits vascular endothelial growth factor-induced endothelial cell migration by an inhibitory effect on the Akt/endothelial nitric oxide synthase pathway**. *Circulation* 2001, **103**(16):2102-2107.
25. Amaravadi R, Thompson CB: **The survival kinases Akt and Pim as potential pharmacological targets**. *J Clin Invest* 2005, **115**(10):2618-2624.
26. Inoue H, Tanabe T, Umesono K: **Feedback control of cyclooxygenase-2 expression through PPARgamma**. *J Biol Chem* 2000, **275**(36):28028-28032.
27. Ricote M, Li AC, Willson TM, Kelly CJ, Glass CK: **The peroxisome proliferator-activated receptor-gamma is a negative regulator of macrophage activation**. *Nature* 1998, **391**(6662):79-82.
28. Robbesyn F, Salvayre R, Negre-Salvayre A: **Dual role of oxidized LDL on the NF-kappaB signaling pathway**. *Free Radic Res* 2004, **38**(6):541-551.
29. Wang XF, Zhang JY, Li L, Zhao XY, Tao HL, Zhang L: **Metformin improves cardiac function in rats via activation of AMP-activated protein kinase**. *Clin Exp Pharmacol Physiol* 2011, **38**(2):94-101.
30. Mugabo Y, Mukaneza Y, Renier G: **Palmitate induces C-reactive protein expression in human aortic endothelial cells. Relevance to fatty acid-induced endothelial dysfunction**. *Metabolism* 2011, **60**(5):640-648.
31. Zou MH, Hou XY, Shi CM, Nagata D, Walsh K, Cohen RA: **Modulation by peroxynitrite of Akt- and AMP-activated kinase-dependent Ser1179 phosphorylation of endothelial nitric oxide synthase**. *J Biol Chem* 2002, **277**(36):32552-32557.
32. Eid AA, Ford BM, Block K, Kasinath BS, Gorin Y, Ghosh Choudhury G, Barnes JL, Abboud HE: **AMPK negatively regulates NOX4-dependent activation of p53 and epithelial cell apoptosis in diabetes**. *J Biol Chem* 2010.
33. Alba G, El Bekay R, Alvarez-Maqueda M, Chacon P, Vega A, Monteseirin J, Santa Maria C, Pintado E, Bedoya FJ, Bartrons R *et al*: **Stimulators of AMP-activated protein kinase inhibit the respiratory burst in human neutrophils**. *FEBS Lett* 2004, **573**(1-3):219-225.
34. Kliewer SA, Umesono K, Noonan DJ, Heyman RA, Evans RM: **Convergence of 9-cis retinoic acid and peroxisome proliferator signalling pathways through heterodimer formation of their receptors**. *Nature* 1992, **358**(6389):771-774.
35. Hu E, Kim JB, Sarraf P, Spiegelman BM: **Inhibition of adipogenesis through**

MAP kinase-mediated phosphorylation of PPARgamma. *Science* 1996, **274**(5295):2100-2103.

36. Moon L, Jun MS, Kim YM, Lee YS, Kim HJ, Seo HG, Lee JH, Son KH, Lee DH, Kim YS *et al*: **7,8-didehydrocimigenol from Cimicifugae rhizoma inhibits TNF-alpha-induced VCAM-1 but not ICAM-1expression through upregulation of PPAR-gamma in human endothelial cells**. *Food Chem Toxicol* 2010.
37. Chiba Y, Ogita T, Ando K, Fujita T: **PPARgamma ligands inhibit TNF-alpha-induced LOX-1 expression in cultured endothelial cells**. *Biochem Biophys Res Commun* 2001, **286**(3):541-546.
38. Chen XP, Zhang TT, Du GH: **Lectin-like oxidized low-density lipoprotein receptor-1, a new promising target for the therapy of atherosclerosis?** *Cardiovasc Drug Rev* 2007, **25**(2):146-161.
39. Baldwin AS, Jr.: **The NF-kappa B and I kappa B proteins: new discoveries and insights**. *Annu Rev Immunol* 1996, **14**:649-683.
40. Springer TA: **Traffic signals for lymphocyte recirculation and leukocyte emigration: the multistep paradigm**. *Cell* 1994, **76**(2):301-314.
41. Hattori Y, Suzuki K, Hattori S, Kasai K: **Metformin inhibits cytokine-induced nuclear factor kappaB activation via AMP-activated protein kinase activation in vascular endothelial cells**. *Hypertension* 2006, **47**(6):1183-1188.
42. Gauvin A, Pinguet F, Poujol S, Astre C, Bressolle F: **High-performance liquid chromatographic determination of vinorelbine in human plasma and blood: application to a pharmacokinetic study**. *J Chromatogr B Biomed Sci Appl* 2000, **748**(2):389-399.

Figure

Click here to download Figure: figure2011.pptx

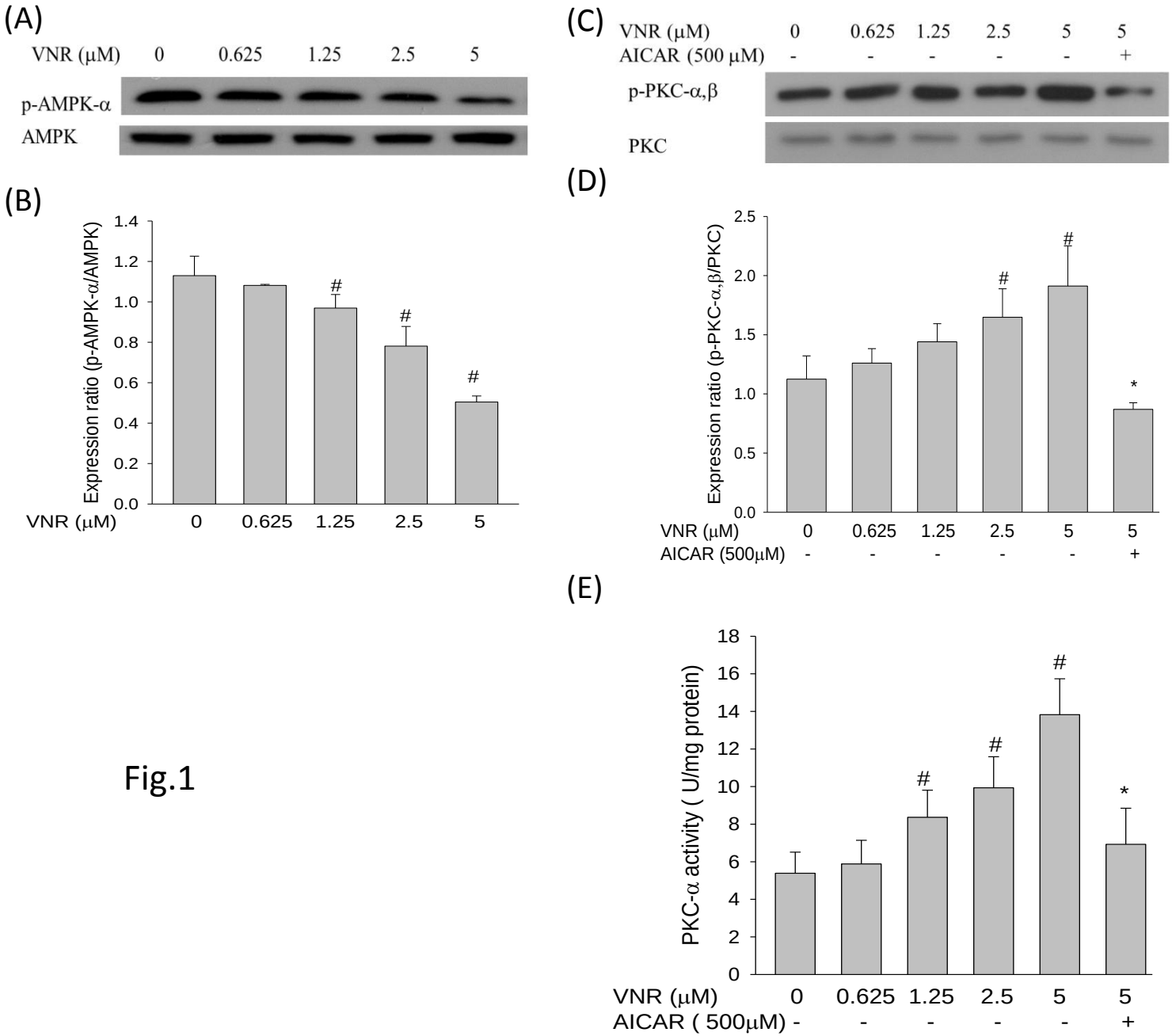

Fig.1

(A)

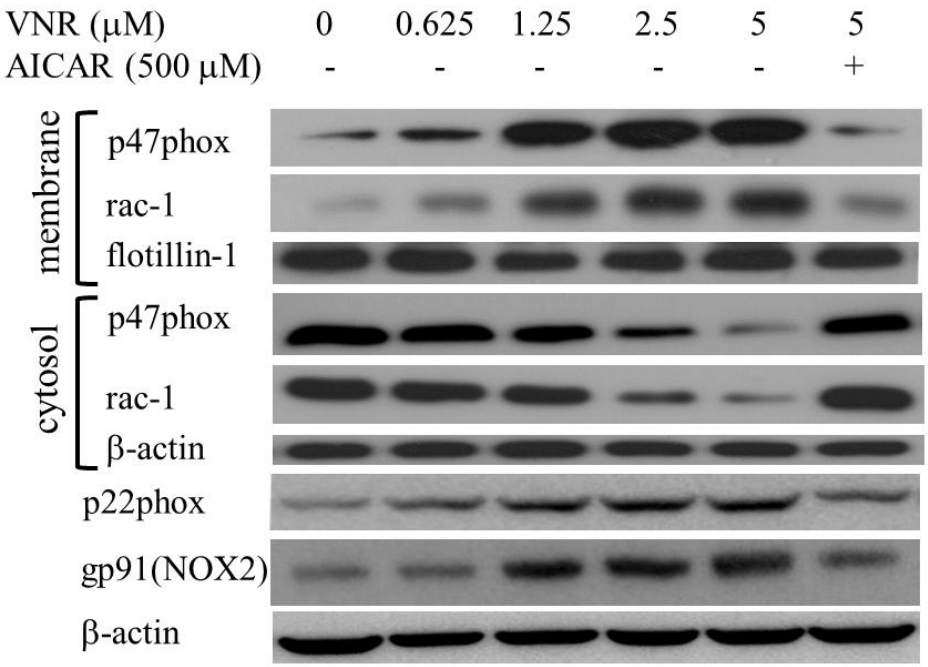
VNR (μM) 0 0.625 1.25 2.5 5 5
AICAR (500 μM) - - - - - +
membrane
p47phox
rac-1
flotillin-1
cytosol
p47phox
rac-1
β-actin
p22phox
gp91(NOX2)
β-actin

Fig.2

(B)

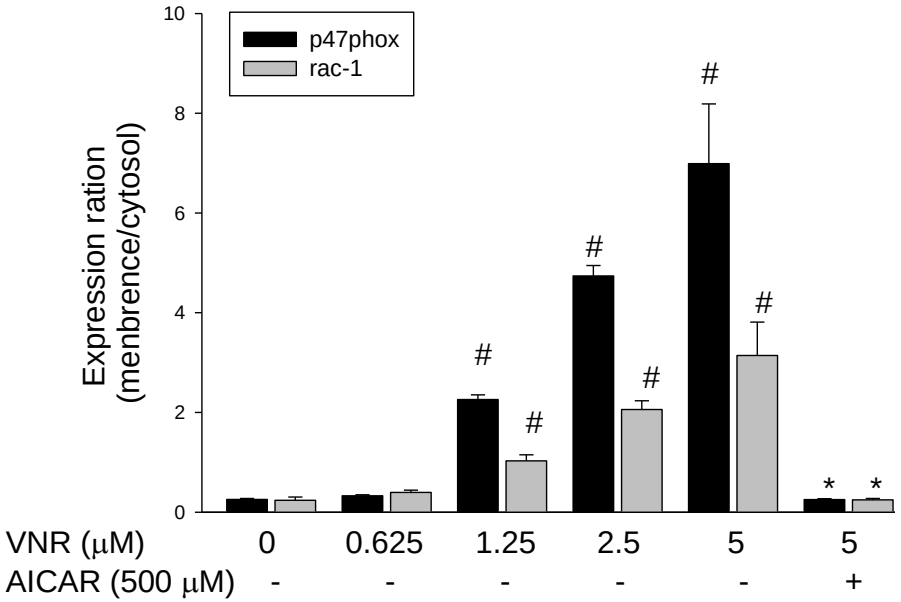
p47phox
rac-1
Expression ration
(menbrence/cytosol)
VNR (μM) 0 0.625 1.25 2.5 5 5
AICAR (500 μM) - - - - - +

(C)

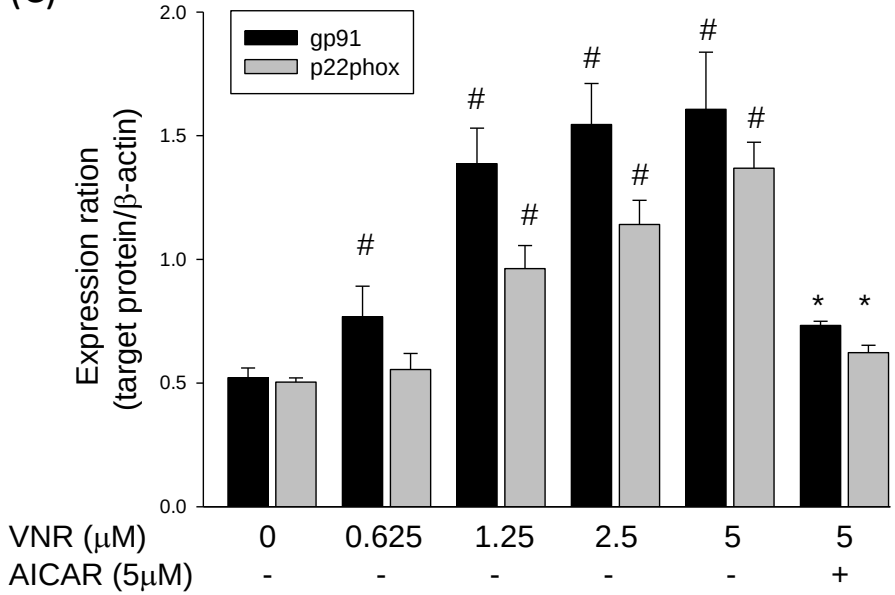
gp91
p22phox
Expression ration
(target protein/β-actin)
VNR (μM) 0 0.625 1.25 2.5 5 5
AICAR (5μM) - - - - - +

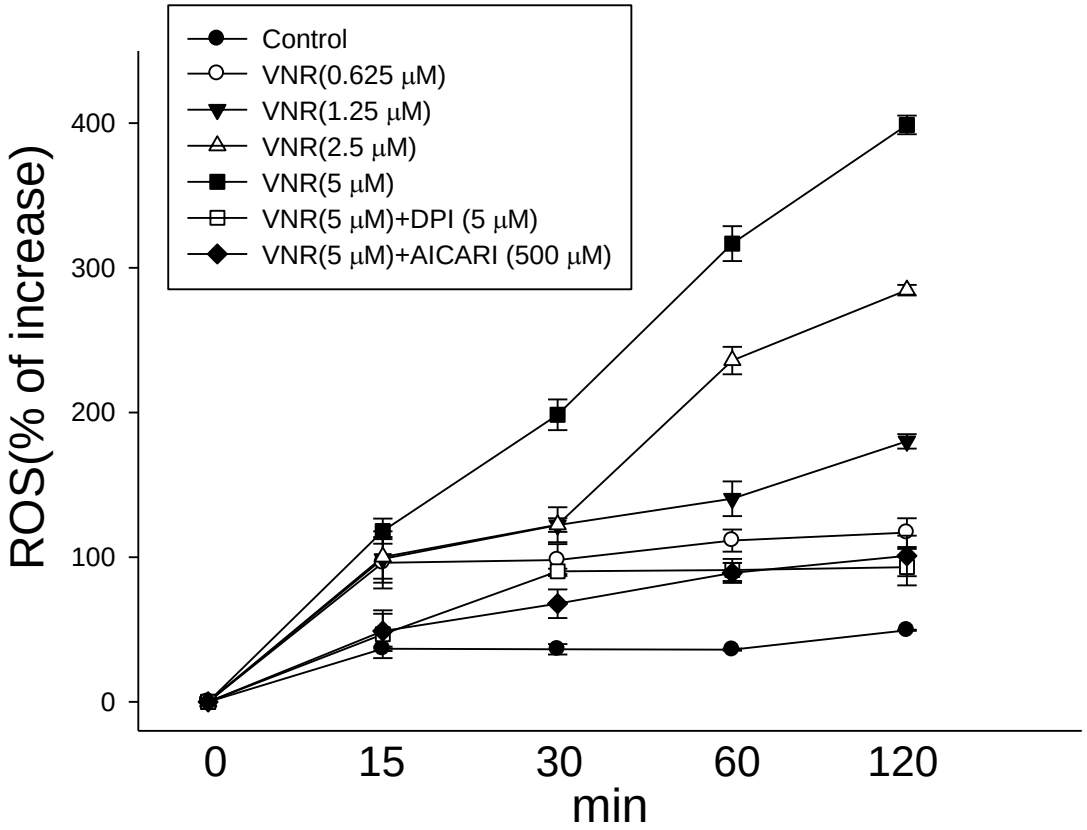
Control
VNR(0.625 μM)
VNR(1.25 μM)
VNR(2.5 μM)
VNR(5 μM)
VNR(5 μM)+DPI (5 μM)
VNR(5 μM)+AICARI (500 μM)
ROS(% of increase)
0
100
200
300
400
0
15
30
60
120
min

Fig.3

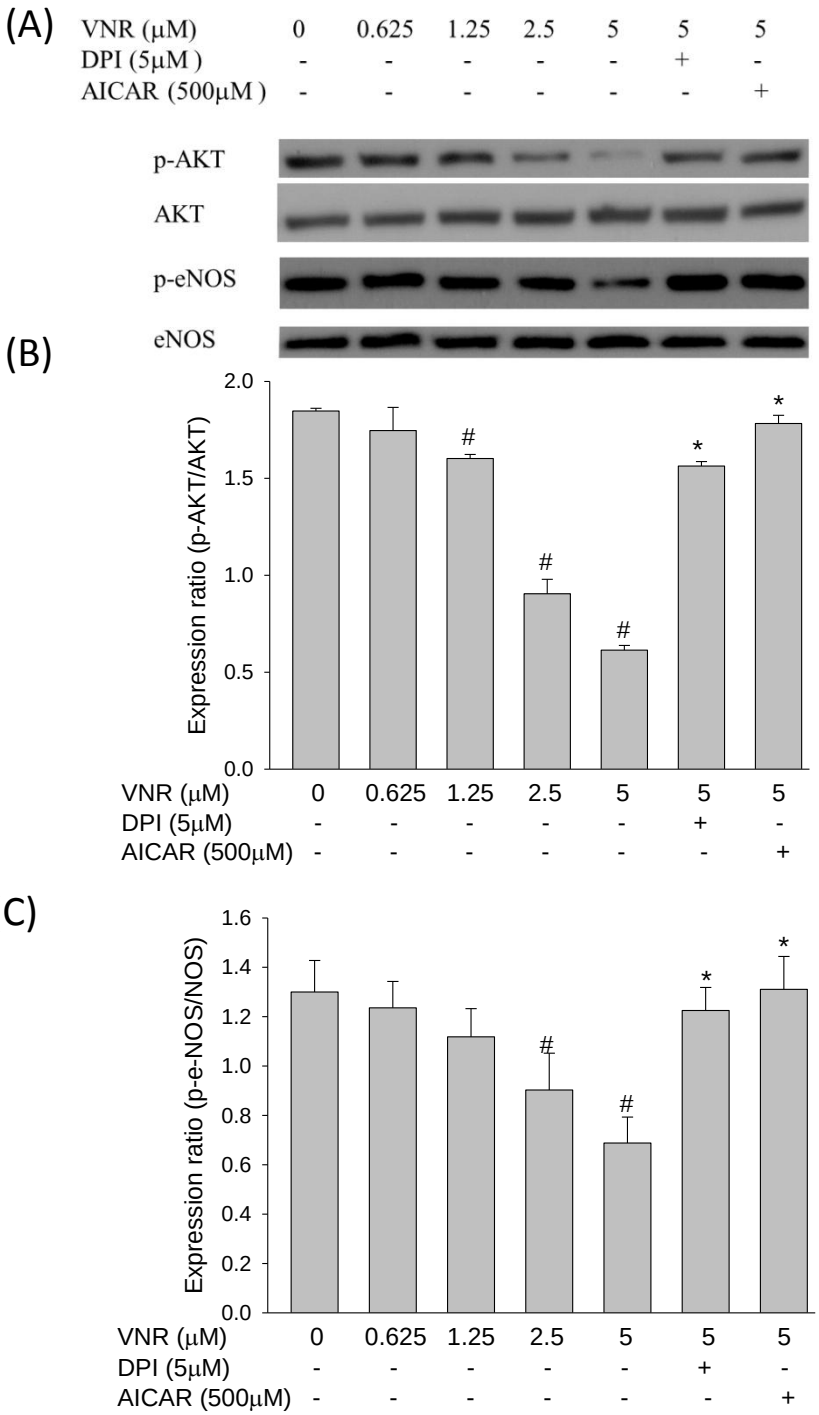
(A)
VNR (μM) 0 0.625 1.25 2.5 5 5 5
DPI (5μM) - - - - - + -
AICAR (500μM) - - - - - - +
p-AKT
AKT
p-eNOS
eNOS
(B)
Expression ratio (p-AKT/AKT)
2.0
1.5
1.0
0.5
0.0
#
#
#
*
*
VNR (μM) 0 0.625 1.25 2.5 5 5 5
DPI (5μM) - - - - - + -
AICAR (500μM) - - - - - - +
(C)
Expression ratio (p-e-NOS/NOS)
1.6
1.4
1.2
1.0
0.8
0.6
0.4
0.2
0.0
#
#
*
*
VNR (μM) 0 0.625 1.25 2.5 5 5 5
DPI (5μM) - - - - - + -
AICAR (500μM) - - - - - - +

Fig.4

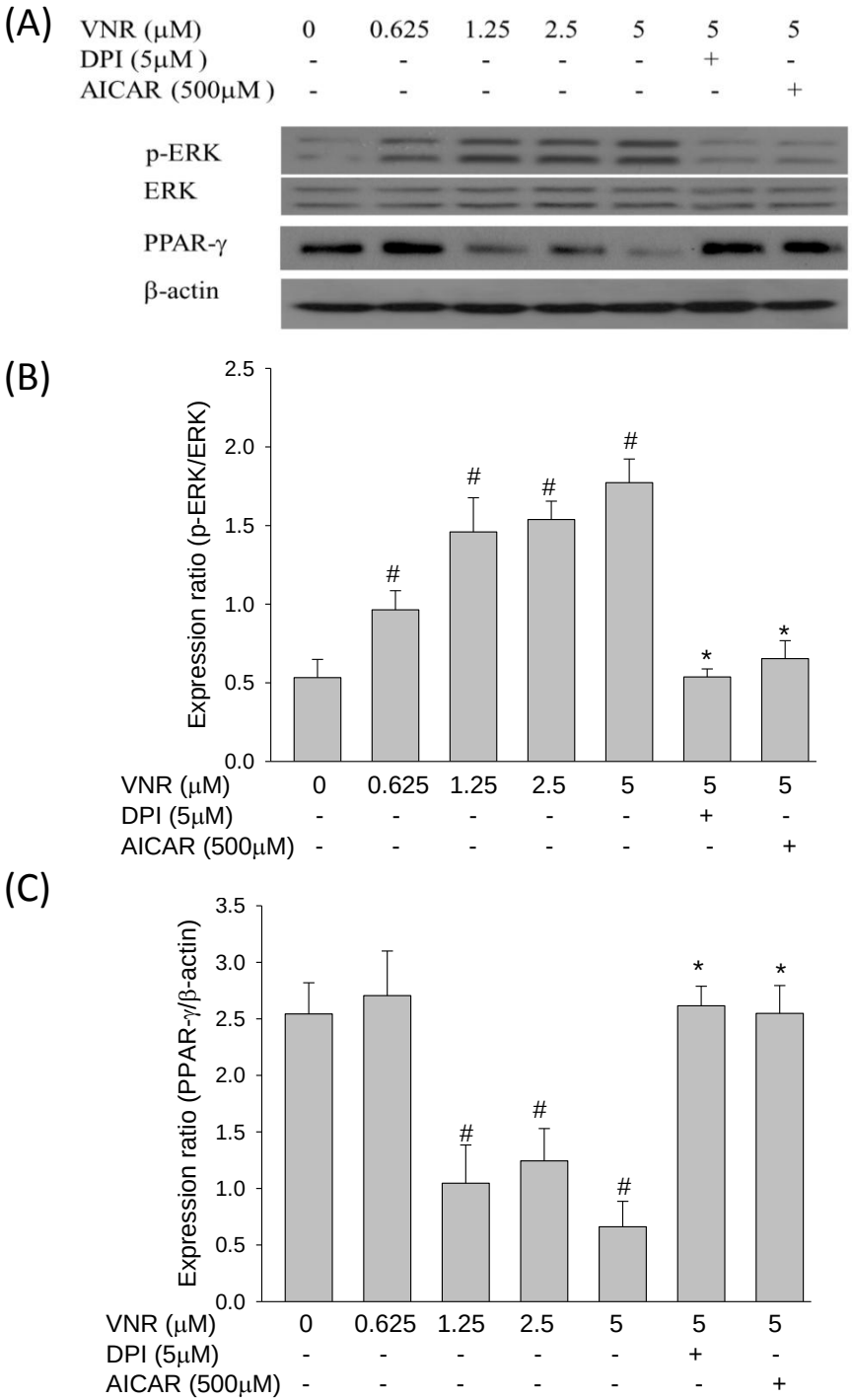
(A)
VNR (μM) 0 0.625 1.25 2.5 5 5 5
DPI (5μM) - - - - - + -
AICAR (500μM) - - - - - - +
p-ERK
ERK
PPAR-γ
β-actin
(B)
Expression ratio (p-ERK/ERK)
2.5
2.0
1.5
1.0
0.5
0.0
#
#
#
#
*
*
VNR (μM) 0 0.625 1.25 2.5 5 5 5
DPI (5μM) - - - - - + -
AICAR (500μM) - - - - - - +
(C)
Expression ratio (PPAR-γ/β-actin)
3.5
3.0
2.5
2.0
1.5
1.0
0.5
0.0
#
#
#
*
*
VNR (μM) 0 0.625 1.25 2.5 5 5 5
DPI (5μM) - - - - - + -
AICAR (500μM) - - - - - - +

Fig.5

(A)

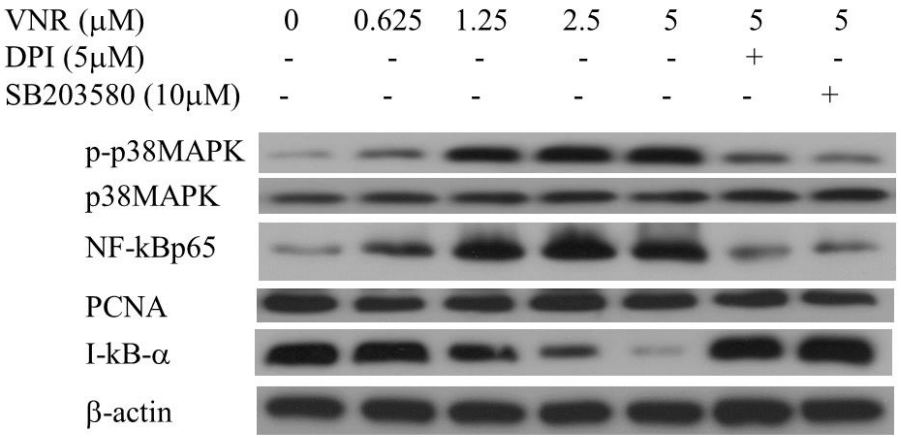
VNR (μM) 0 0.625 1.25 2.5 5 5 5
DPI (5μM) - - - - - + -
SB203580 (10μM) - - - - - - +
p-p38MAPK
p38MAPK
NF-kBp65
PCNA
I-kB-α
β-actin

(C)

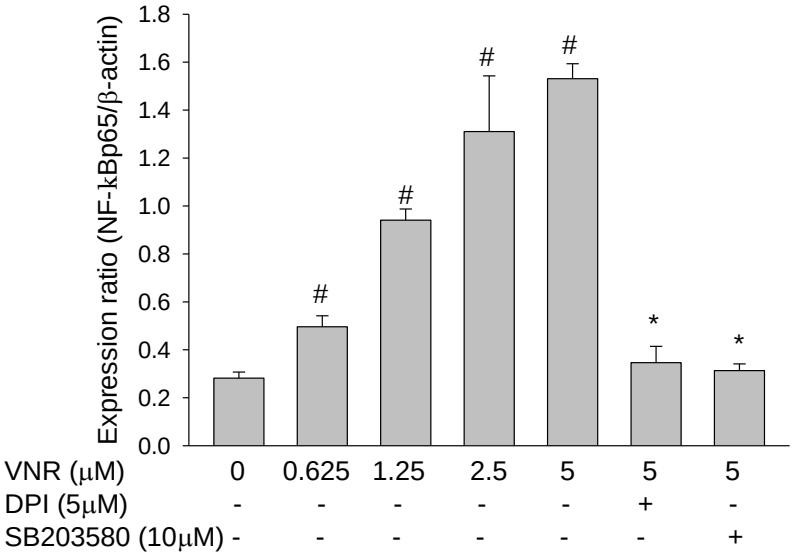
Expression ratio (NF-kBp65/β-actin)
1.8
1.6
1.4
1.2
1.0
0.8
0.6
0.4
0.2
0.0
* *
VNR (μM) 0 0.625 1.25 2.5 5 5 5
DPI (5μM) - - - - - + -
SB203580 (10μM) - - - - - - +

(B)

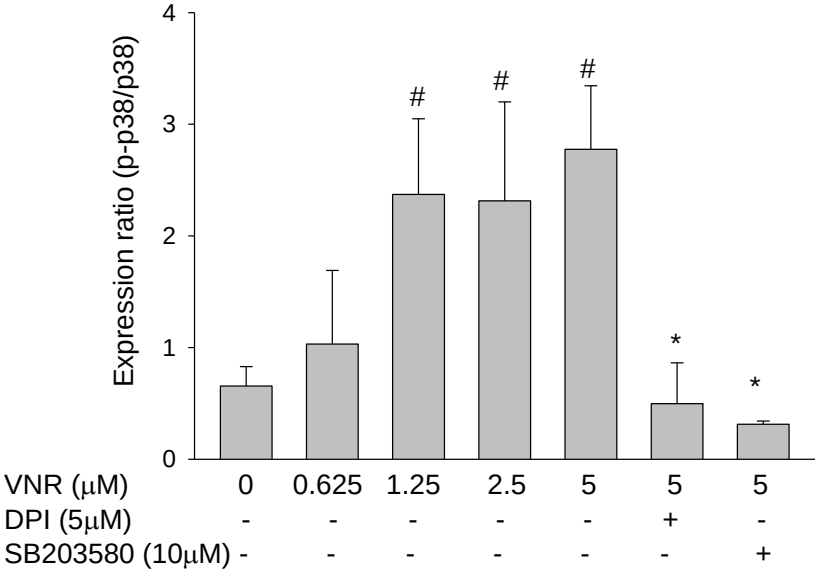
Expression ratio (p-p38/p38)
4
3
2
1
0
* *
VNR (μM) 0 0.625 1.25 2.5 5 5 5
DPI (5μM) - - - - - + -
SB203580 (10μM) - - - - - - +

(D)

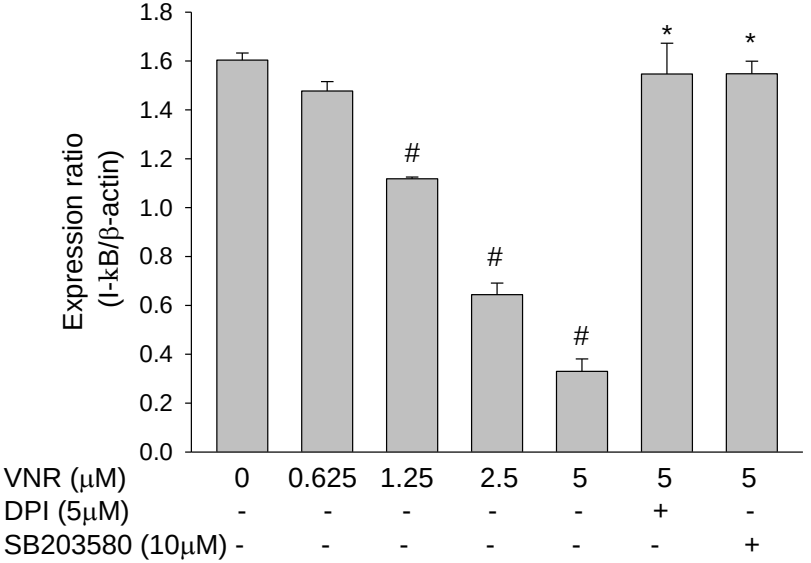
Expression ratio (I-kB/β-actin)
1.8
1.6
1.4
1.2
1.0
0.8
0.6
0.4
0.2
0.0
* *
VNR (μM) 0 0.625 1.25 2.5 5 5 5
DPI (5μM) - - - - - + -
SB203580 (10μM) - - - - - - +

Fig.6

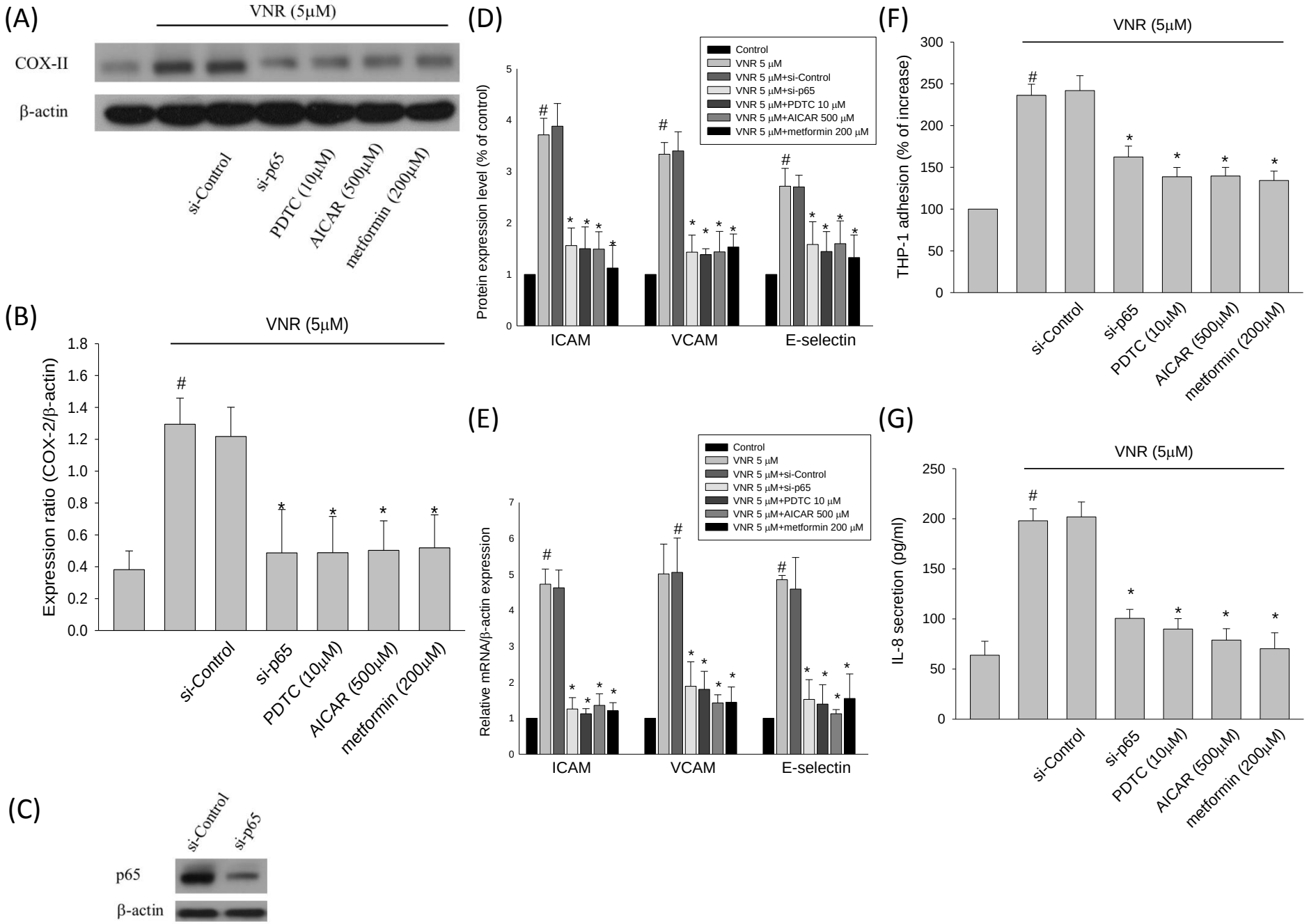
(A)
VNR (5μM)
COX-II
β-actin
si-Control
si-p65
PDTC (10μM)
AICAR (500μM)
metformin (200μM)
(B)
VNR (5μM)
Expression ratio (COX-2/β-actin)
(C)
si-Control
si-p65
p65
β-actin
(D)
Protein expression level (% of control)
Control
VNR 5 μM
VNR 5 μM+si-Control
VNR 5 μM+si-p65
VNR 5 μM+PDTC 10 μM
VNR 5 μM+AICAR 500 μM
VNR 5 μM+metformin 200 μM
ICAM
VCAM
E-selectin
(E)
Relative mRNA/β-actin expression
(F)
VNR (5μM)
THP-1 adhesion (% of increase)
(G)
VNR (5μM)
IL-8 secretion (pg/ml)

Fig.7

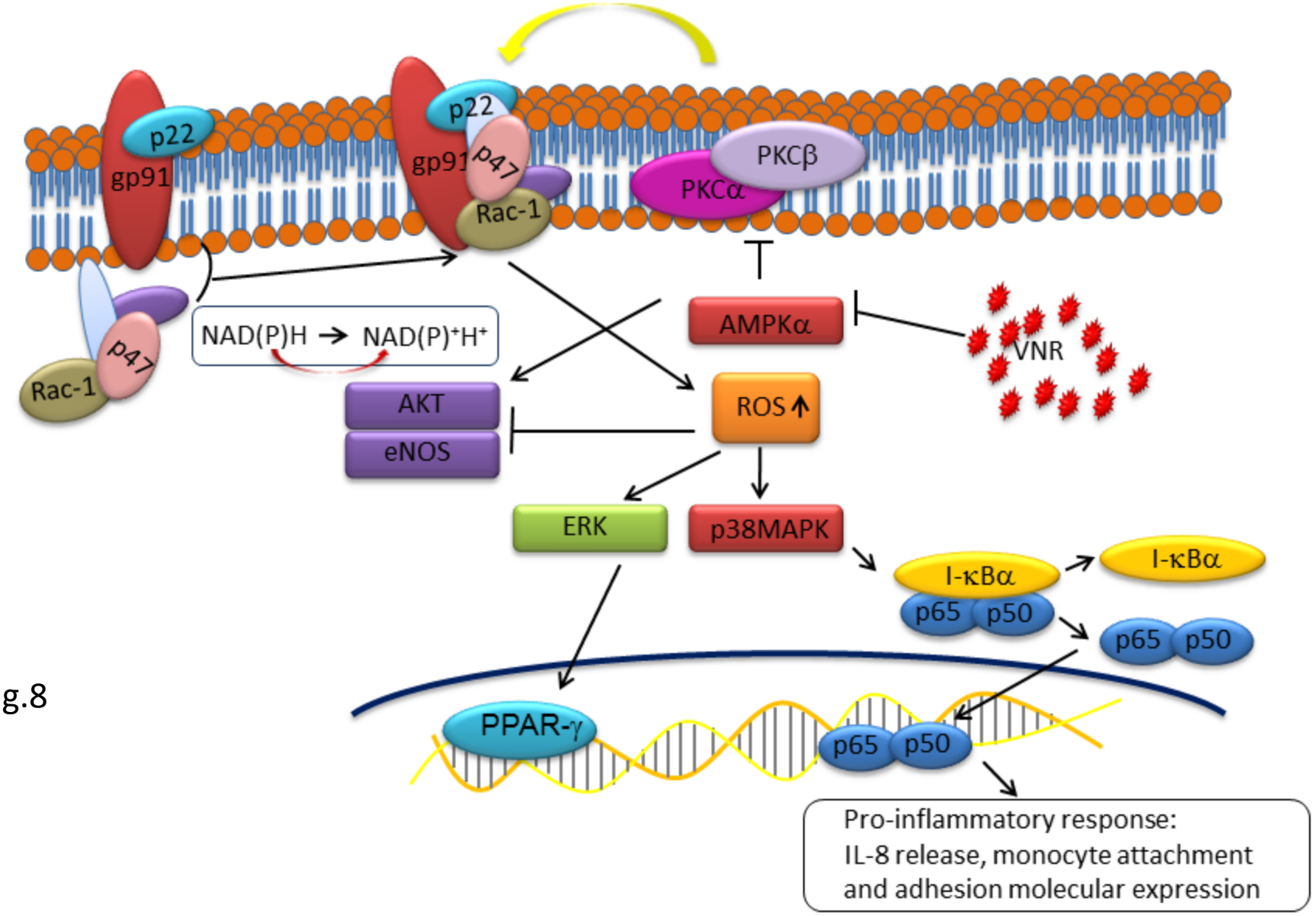
p22
gp91
p47
Rac-1
p22
gp91
p47
Rac-1
PKCβ
PKCα
AMPKα
VNR
NAD(P)H → NAD(P)⁺H⁺
AKT
eNOS
ROS
ERK
p38MAPK
I-κBα
I-κBα
p65
p50
p65
p50
PPAR-γ
p65
p50
Pro-inflammatory response:
IL-8 release, monocyte attachment
and adhesion molecular expression

Fig.8